Landfast ice thickness in the Canadian Arctic Archipelago from Observations and Models

Stephen. E. L. Howell[1], Frédéric Laliberté[1], Ron Kwok[2], Chris Derksen[1] and Joshua King[1]

[1]Climate Research Division, Environment and Climate Change Canada, Toronto, Canada

[2]Jet Propulsion Laboratory, California Institute of Technology, Pasadena, California, USA

Abstract

Observed and modelled landfast ice thickness variability and trends spanning more than five decades within the Canadian Arctic Archipelago (CAA) are summarized. The observed sites (Cambridge Bay, Resolute, Eureka and Alert) represent some of the Arctic's longest records of landfast ice thickness. Observed end-of-winter (maximum) trends of landfast ice thickness (1957-2014) were statistically significant at Cambridge Bay (-4.31±1.4 cm decade^{-1}), Eureka (-4.65±1.7 cm decade^{-1}) and Alert (-4.44±1.6 cm decade^{-1}) but not at Resolute. Over the 50+ year record, the ice thinned by ~0.24-0.26 m at Cambridge Bay, Eureka and Alert with essentially negligible change at Resolute. Although statistically significant warming in spring and fall was present at all sites, only low correlations between temperature and maximum ice thickness were present; snow depth was found to be more strongly associated with the negative ice thickness trends. Comparison with multi-model simulations from Coupled Model Intercomparison project phase 5 (CMIP5), Ocean Reanalysis Intercomparison (ORA-IP) and Pan-Arctic Ice-Ocean Modeling and Assimilation System (PIOMAS) show that although a subset of current generation models have a 'reasonable' climatological representation of landfast ice thickness and distribution within the CAA, trends are unrealistic and far exceed observations by up to two orders of magnitude. ORA-IP models were found to have positive correlations between temperature and ice thickness over the CAA, a feature that is inconsistent with both observations and coupled models from CMIP5.

1. Introduction

The World Meteorological Organization (WMO, 1970) defines landfast sea ice as "sea ice which remains fast along the coast, where it is attached to the shore, to an ice wall, to an ice front, or over shoals, or between grounded icebergs." In the Arctic, this ice typically extends to the 20-30 m isobaths [*Mahoney et al.,* 2007; *Mahoney et al.,* 2014]. It melts each summer and reforms in the fall but there are regions along the northern coast of the Canadian Arctic Archipelago (CAA) where multi-year landfast ice (also termed an "ice plug") is present. The two most prominent regions of multi-year landfast sea ice in the CAA are located in Nansen Sound and Sverdrup Channel [*Serson,* 1972; *Serson,* 1974] (Figure 1). It has been documented that ice remained intact from 1963-1998 in Nansen Sound and from 1978-1998 in Sverdrup Channel [*Jeffers et al.,* 2001; *Melling,* 2002; *Alt et al.,* 2006]. The extreme warm year of 1998 disintegrated the ice in both regions and their survival during the summer melt season in recent years has occurred less frequently [*Alt et al.,* 2006]. Over the entire Arctic, landfast ice extent is declining at 7% decade^{-1} since the mid-1970s [*Yu et al.,* 2013]

Records of landfast ice thickness provide annual measures of ice growth that can also almost entirely be attributed to atmospheric forcing with negligible deep ocean influence on local ice formation. While the key forcings on landfast ice and offshore ice are different, the seasonal behavior of landfast ice can nevertheless provide useful information for understanding the interannual variability of ice thickness in both regimes. Presently, there is no pan-Arctic network for monitoring changes in landfast ice but available measurements suggest thinning in recent years. Thickness measurements near Hopen, Svalbard revealed thinning of landfast ice in the Barents Sea region by 11 cm decade^{-1} between 1966 and 2007 [*Gerland et al.,* 2008]. From a composite time series of landfast ice thickness from 15 stations along the Siberian coast,

47 *Polyakov et al.* [2010] estimate an average rate of thinning of 3.3 cm decade^{-1} between the mid-
48 1960s and early 2000s. Relatively recent observations by *Mahoney et al.* [2007] and
49 *Druckenmiller et al.* [2009] found longer ice-free seasons and thinner landfast ice compared to
50 earlier records.

51 At four sites in the CAA, *Brown and Cote* [1992] (hereinafter, BC92) provided the first
52 examination of the interannual variability of end-of-winter (maximum) landfast ice thickness and
53 associated snow depth over the period 1957-1989. Their results highlighted the insulating role of
54 snow cover in explaining 30-60% of the variance in maximum ice thickness. Similar results were
55 also reported by *Flato and Brown* [1996] and *Gough et al.* [2004]. In the record examined by
56 BC92, no evidence for systematic thinning of landfast ice in the CAA was found. Landfast ice
57 thickness records at several of these CAA sites are now over 50 years in length, which represents
58 an addition of more than two decades of measurements since BC92 during a period that saw
59 dramatic reductions in the extent and thickness of Arctic sea ice [e.g. *Kwok and Rothrock,* 2009;
60 *Stroeve et al.,* 2012].

61 The sparse network of long term observations of snow and ice thickness in the Arctic
62 (clearly exhibited by only four ongoing measurements sites operated by Environment Canada in
63 the CAA) has made the use of models imperative to provide a broader regional scale perspective
64 of sea ice trends in a warming climate. Given the coarse spatial resolution of global climate
65 models, previous studies focusing on the CAA have relied on either a one-dimensional
66 thermodynamic dynamic model [*Flato and Brown*, 1996; *Dumas et al.*, 2006] or a regional three-
67 dimensional ice-ocean coupled model [e.g. *Sou and Flato,* 2009]. Specifically, *Dumas et al.*
68 [2006] found projected maximum ice thickness decreases of 30 cm by 2041-2060 and 50 cm by
69 2081-2100 and *Flato and Sou* [2009] reported a potential 17% decrease in overall ice thickness

throughout the CAA by 2041-2060. However, in recent years some global climate models, reanalysis products, and data assimilation systems are now of sufficient spatial resolution to assess potential landfast ice thickness changes within the CAA.

This analysis examines the trends of measured landfast ice thickness, snow depth and air temperature over a 50+ year period between 1957 and 2014 and compares the results with the earlier analysis by BC92. We then use this observational foundation to evaluate the representativeness of landfast ice in state-of-the-art global climate models, assimilation systems and re-analysis products.

2. Data Description

2.1. Observations

Landfast ice thickness and corresponding snow depth measurement have been made regularly at many coastal stations throughout Canada since about 1950. These data are quality controlled and archived at the Canadian Ice Service (CIS) and represent one of the few available sources of continuous ice thickness measurements in the Arctic. In general, thickness measurements are taken once per week, starting after freeze-up when the ice is safe to walk on and continuing until breakup or when the ice becomes unsafe. Complete details of this dataset are provided by Brown and Cote (1992). The dataset is available on the CIS web site (http://www.ec.gc.ca/glaces-ice/, see Archive followed by Ice Thickness Data). Four sites in the CAA were selected for study: Alert, Eureka, Resolute, and Cambridge Bay (Figure 1). Although there are other sites in the database, these sites are the only ones than span the same 55-year period between 1960 and 2014. The record at Mould Bay, used in BC92, terminated in the early 1990s. Together these sites cover ~20° in latitude (Figure 1) that are adjacent to an area of thick

Arctic sea ice that experienced the highest thinning in recent years [*Kwok and Rothrock*, 2009; *Laxon et al.*, 2013]. Values of maximum or end-of-winter ice thickness and corresponding snow depth during the ice growth season were extracted from the weekly ice and snow thickness data at the selected sites (see supplementary material). As this study is concerned with annual variability in maximum ice thickness, the main period of interest extends from September to late May.

The other source of observed data used in this study was Environment Canada's monthly mean air temperature records at Alert, Eureka, Resolute, and Cambridge Bay for which a complete description is provided by *Vincent et al.* [2012].

2.2. Models

The representation of CAA landfast sea ice thickness within the Coupled Model Intercomparison project phase 5 (CMIP5) is analyzed using the 1850-2005 Historical experiment followed by the 2006-2099 Representative Concentration Pathway 8.5 (RCP85) experiment [*Taylor et al.*, 2012] (Table 1). Monthly sea ice thickness (variable *sit*), sea ice concentration (variable *sic*), 2 meter temperature (variable *tas*) and snow depth (variable *snd*) were used. The CMIP5 data were retrieved from the British Atmospheric Data Centre database and accessed through the Center for Environmental Data Analysis (www.ceda.ac.uk). Ensemble r6i1p1 and r7i1p1 from model EC-EARTH were removed because of corrupted data. We obtain the multi-model mean of trends and their statistical significance at each grid point by creating the distribution of trends through a Monte-Carlo simulation. We use a t-distribution for the interannual variability and build a noise model to account for internal variability as in *Swart et al.* [2014] and *Laliberté et al.* [2016]. We obtain the multi-model mean of Pearson correlations

and their statistical significance by first performing a Fisher transform and then applying the same method as for the trends. The inverse Fisher transform is applied after obtaining the multi-model mean and its significance. See the appendix for a complete description of the method.

We also investigate ice thickness values from a selection of the highest resolution models [*Storto et al.,* 2011; *Forget et al.,* 2015; *Haines et al.,* 2014, *Zuo et al.,* 2015; *Masina et al.,* 2015] from the Ocean Reanalysis Intercomparison (ORA-IP) [*Balsameda et al.,* 2015; *Chevallier et al.,* 2016] (Table 2) and from the Pan-Arctic Ice-Ocean Modeling and Assimilation System (PIOMAS) [*Zhang and Rothrock*, 2003]. Supporting 2 meter temperature data was obtained from ERA-Interim [*Dee et al.,* 2011].

3. Results and Discussion: Observations

3.1. Climatology

The average behavior of landfast ice at the four sites over the 50+ year record is summarized in Table 3. Ice growth, approximately linear through most of the season, slows after March (Figure 2). Ice thickness reaches a maximum of ~2-2.3 m by late May at all sites. Values are consistent with that reported by BC92 and with recent observations of *Melling et al.* [2015] and *Haas and Howell* [2015]. The standard deviations are nearly uniform (at ~0.2 m) across all sites, giving a relatively low coefficient of variation (CV; a measure of relative dispersion defined as the ratio of the standard deviation to the mean) of ~0.1. The thickest ice is found in Eureka with a 1957-2014 mean of 2.27 m, which is likely due to climatologically lower air temperatures in the fall and winter (Table 3).

Snow depth also appears to grow linearly through the season, peaking in May but unlike ice thickness the monthly variability is high (CV ~0.4) (Figure 3). Mean October to May snow

depths at Resolute, Eureka and Alert range from ~18-23 cm compared to only ~8 cm at Cambridge Bay (Table 3). The rapid buildup of the snow cover due to storms in the fall and early winter that is evident over the Arctic Ocean multi-year ice cover [*Warren et al.,* 1999; *Webster et al.,* 2014], is not seen in these snow depth records within the CAA. The linear behavior in snow depth is likely maintained by continuous wind-driven redistribution and densification throughout the ice growth season [BC92; *Woo and Heron,* 1989].

3.2. Trends

The time series of maximum ice thickness at Cambridge Bay, Resolute, Eureka and Alert are illustrated in Figure 4 and summarized in Table 1. Statistically significant (95% or greater confidence level) negative maximum ice thickness trends are present at Cambridge Bay (-4.31±1.4 cm decade^{-1}), Eureka (-4.65±1.7 cm decade^{-1}) and Alert (-4.44±1.6 cm decade^{-1}) (Table 1). A slight negative trend is present at Resolute but not statistically significant at the 95% confidence level (Table 1). Over the 50+ year record, the ice thinned by ~0.24-0.26 m at Cambridge Bay, Eureka and Alert with essentially negligible change at Resolute. These trends in the CAA are similar to trends on the Siberian coast (-3.3 cm decade^{-1}) [*Polyakov et al.*, 2010] but lower in magnitude compared to the Barents Sea (-11 cm decade^{-1}) [*Gerland et al.,* 2008].

For the shorter record (late 1950s–1989, ~30 years) investigated by BC92 there was a negative trend at Alert (-7.1 cm decade^{-1}), no evidence of a trend at Eureka, and a positive trend at Resolute (10 cm decade^{-1}) but only the positive trend at Resolute was statistically significant at the 95% or greater confidence level. Our results from the present 50+ year record suggest that the negative trend at Alert is robust and the trend at Eureka is now negative and significant. The trend at Resolute is now slightly negative however it is not statistically significant.

Typically, ice thickness reaches its maximum in late May with trends toward earlier dates of maximum ice thickness present at all sites (significant at Resolute, Eureka and Alert; Table 3). The significant trends are between -2.0±0.1 days decade^{-1} at Eureka to -6.2±1.5 days decade^{-1} at Resolute. At Resolute, the date of maximum ice thickness is now on average more than a month earlier than the early 1960's although this is not reflected in the trend in ice thickness. Freeze onset at these sites is also increasing at ~3-6 days decade^{-1} [*Howell et al.,* 2009] and demonstrates a shortened growth season at Resolute, Eureka and Alert. Together, the trends of ice thickness and their recorded dates suggest a systematic thinning of landfast ice at Cambridge Bay, Eureka and Alert.

3.3. Ice thickness linkages with snow depth and temperature

The variability of landfast thickness at these Arctic sites was previously found to be largely driven by interannual variations in snow depth and air temperature [BC92; *Flato and Brown*, 1996]. With the 50+ year record at the four sites, we can examine the corresponding linkages to snow depth and temperature.

For snow depth, the only trend that is statistically significant at the 95% confidence is Cambridge Bay at -0.8±0.4 cm decade^{-1} (Table 3). In contrast, BC92 found a significant positive trend at Alert (4 cm decade^{-1}), a trend of low significance in Eureka, and a negative and significant trend at Resolute (-3.3 cm decade^{-1}). Looking at the detrended correlations (r) between snow depth and ice thickness reveals the strongest correlation at Resolute (r=-0.71) followed by Eureka (r=-0.66), Alert (r=-0.47) and Cambridge Bay (r=-0.31). Figure 6 provides evidence from extreme years of the role of deeper snow inhibiting ice growth compared to thinner snow, but the positive trends in snow thickness are not significant at Resolute, Eureka

185 and Alert. This may in part be due to the single pointwise snow depth and ice thickness
186 measurements made at each point in time, which fail to capture spatial heterogeneity in the snow
187 depth/ice thickness relationship.

188 With respect to observed temperature, we find significant warming trends in the spring
189 and fall at all sites over the 50+ year record (Table 3; Figure 7). Significant warming is also
190 present at all sites in the summer except Resolute and at all sites during the winter except Eureka
191 (Table 3). Warming is highest during the fall, at ~0.6°C decade^{-1} at all sites (Table 3). The
192 detrended correlation between temperature (winter, spring, summer and autumn) and maximum
193 ice thickness is weak at all sites. For example, the strongest detrended correlation between
194 maximum ice thickness and temperature (winter and spring) is found at Cambridge Bay during
195 the winter and spring but is only ~0.4.

196 Also of interest is that the observed temperature trends over this period differ
197 considerably from the earlier period investigated in BC92, in which they reported cooling at all
198 the sites, with a significant cooling trend at Eureka. It was noted that the general cooling over
199 their record coincided with the 1946-1986 cooling trend over much of the eastern Arctic and
200 northwest Atlantic reported by *Jones et al.* [1987]. This cooling trend halted during the 1980s
201 and the warming, seen in the current and longer record, has resumed [*Jones et al.,* 1999]. Arctic
202 land areas have experienced an overall warming of about ~2°C since the mid-1960s, with area-
203 wide positive temperature anomalies that show systematic changes since the end of the 20th
204 century, which continued through 2014 [J*effries and Richter-Menge,* 2015]. Recently, warming
205 in Canadian Arctic regions was found to be greater than the pan-Arctic trend by up to 0.2°C
206 decade^{-1} [*Tivy et al.,* 2011].
207

4. Results and Discussion: Models

4.1. Climatology

In order to compare seasonal cycles and trends in landfast ice thickness and snow depth between models and observations, we limit our comparison to models with a reasonable representation of the CAA, i.e. those with an open Parry Channel (i.e. bcc-csm-1-1, bcc-csm-1-1m, CNRM-CM5, ACCESS1-0, ACCESS1-3, FIO-ESM, EC-EARTH, inmcm4, MIROC5, MPI-ESM-LR, MPI-ESM-MR, MRI-CGCM3, CCSM4, NorESM1-M, NorESM1-ME, GFDL-CM3, GFDL-ESM2G, GFL-ESM2M, CESM1-BCG, CESM1-CAM5, CESM-WACCM). In these models, sufficient spatial resolution allows us to find sample points that are almost collocated to *in situ* observation locations. The sample points were determined by finding the closest ocean grid point where the sea ice is packed for a good portion of the year, but not all year. Grid points with this characteristic therefore share the most important feature of the landfast ice at our observations locations: it is not perennial. Mathematically, we sought sample points where the sea ice concentration is on average above 85% for more than one month but less than 11 months over the 1955-2014 period. The Eureka site is however particularly challenging for models because it lies deep in a very narrow channel, which is only resolved by the MPI-ESM-MR in the CMIP5. As a result, for most models, the sample point for Eureka is located on the western shore of Ellesmere Island. This is a consequence of using samples as some models either do not resolve some of the channels in the CAA or have too perennial packed ice cover (e.g. CESM1-CAM5), then the sample points are further from the observational site than would be desired. We chose to use sample points in our comparison to observations instead of using regional averages for two main reasons. The first reason is that using regional averages would have lumped together different ice dynamics regimes that should not necessarily be expected to compare well

to point observations on landfast ice. The second reason is that we are of the opinion that the resolution in many of these models is sufficiently high to warrant such a direct comparison and provides a better benchmark than regional averages for landfast ice modelling in the CAA.

The seasonal cycle (1955-2014) of median ice thickness from CMIP5 (black), ORA-IP models CGLORS, ORAP5.0 and GLORYS2V3 (blue), ECCO-v4 (green) and UR025.4 (red) is shown in Figure 8. ORA-IP models have been split into three groups based, respectively, on their high, medium and low ice thicknesses at Alert. Ice thickness from CMIP5 is comparable to observations (Figure 2) at Cambridge Bay and Resolute with maximum ice thickness reaching 200 cm. The ORA-IP models are less consistent. ECCO-v4 tends to have thicker sea ice than observations at Cambridge Bay, Resolute and Eureka but thinner at Alert. CGLORS, ORAP5.0, and GLORYS2V3, on the other hand, are comparable to observations at Cambridge Bay, Resolute and Eureka but have extremely thick and perennial ice close to Alert.

The seasonal cycle (1955-2014) of median snow depth from CMIP5 is shown in Figure 9. CMIP5 models indicate a linear increase similar to observations reaching a maximum of ~20 cm in April or May. This is lower than the observed maximum at Resolute, Eureka and Alert but is about twice as much as at Cambridge Bay. While the snow depth reaches zero during the summer at Eureka and Alert in models, the sea ice thickness does not (Figure 8), unlike in observations. This likely reflects the fact that the grid cell thickness in sea ice models with thickness classes a represents the average thickness over these classes. In August the thinner ice classes might have melted but thicker ice classes can still be found, resulting in a substantial average ice thickness over the grid cell. The seasonal cycle over packed ice in these models thus gives a reasonable representation of the seasonal cycle over landfast ice in the CAA, especially in the southern region of the CAA. Overall, this comparison shows how recent improvements in

sea ice model resolution allows comparisons with observations that required dynamical downscaling techniques in the previous generation of sea ice models [i.e. *Dumas et al. 2005; Sou and Flato, 2013*].

Despite relatively high spatial resolution, PIOMAS does not resolve seasonal ice thickness along the coasts and within the very narrow channels within the CAA (not shown). As a result, Cambridge Bay and Resolute Bay sites represent the only long-term monitoring sites within the CAA suitable for comparison since PIOMAS. The monthly time series of PIOMAS ice and snow thickness estimates at Cambridge Bay and Resolute is shown in Figure 10. The seasonal cycle of ice growth at Cambridge Bay and Resolute is representative compared to observations (Figure 2) but PIOMAS estimates retain more ice in August and September, particularly at Resolute. Ice growth reaches a maximum in April at Cambridge and in May at Resolute which is 1-month earlier compared to observations. Snow depth follows a linear increase similar to observations (Figure 3) with good agreement at Cambridge Bay but considerably underestimates snow depth at Resolute (Figure 10). *Schweiger et al.* [2011] performed a detailed comparison of PIOMAS ice thickness values against *in situ* and Ice, Cloud, and land Elevation Satellite (ICESat) ice thickness observations and found strong correlations. They determined a root mean square error (RMSE) of ~0.76 m and noted that PIOMAS generally overestimates thinner ice and underestimates thicker ice. At both sites within the CAA, PIOMAS ice thickness data is in reasonably good agreement with *in situ* observations with RMSE's of 0.29 cm at Cambridge Bay and 0.68 cm at Resolute (Figure 11). The systematic overestimate of thinner ice reported by *Schweiger et al.* [2011] is more apparent at Resolute than Cambridge Bay (Figure 11). The higher latitude regions of the CAA where there is an intricate

mix of seasonal first-year ice and multi-year ice is a problem for PIOMAS and thus contributes to the larger discrepancy at Resolute compared to Cambridge Bay.

4.2. Trends

The spatial distribution of maximum sea ice thickness trends from ORA-IP and CMIP5 is illustrated in Figures 12. The CMIP5 model-mean exhibit a fairly uniform trend pattern, consistent with the different in situ observations (Figure 4) but with overestimated negative thickness trends. Although, for individual models this pattern is far from uniform, the general pattern and magnitude of thickness trends tend to be roughly in accordance with temperature trends (not shown). A similar behavior is observed in the ORA-IP models, with the notable exception of CGLORS, where positive thickness trends are found almost everywhere (Figure 12a). This is robust and it appears that the model is not completely equilibrated in the CAA and exhibit large month-to-month adjustments. Model ORAP5.0 also is not completely equilibrated in the region for years 1979-1984. During those years, it exhibits large inter annual changes in thickness. For this reason, we are only considering years 1985-2013 for this model.

For PIOMAS, the North-South overestimated trend is also present (not shown) as with CMIP5 and ORA-IP. Looking specifically at trends computed from 1979-2014 near the observed sites indicates that the mean maximum ice thickness linear trend from at Cambridge Bay is -13.4+3.4 cm decade^{-1} which is almost double the observational trend of 6.2±2.4 cm decade^{-1}. At Resolute, the PIOMAS linear trend is 24.0±4.1 cm decade^{-1} which is considerably stronger than the observational trend of -4.9±3.51 cm decade^{-1}.

4.3. Ice thickness linkages with snow depth and temperature

Even though ORA-IP models have unrealistically large thickness trends, the pattern of inter annual correlation (detrended) between winter temperatures and thicknesses is roughly consistent across models (Figure 13). Some ORA-IP models also experience positive correlations (e.g. CGLORS, ORAP5.0, GLORYS2V3 and UR025.4) that are mostly located north of the CAA or within the CAA in regions where multi-year ice is known to be present. It is possible that warmer temperatures are associated with an increased flux of thicker multi-year ice into the CAA which is known to occur [e.g. *Howell et al.*, 2013] but the driving processes responsible for these positive correlations require more investigation. In CMIP5 models, no model exhibits positive correlations with temperature that resemble ORA-IP models over the CAA. Although the time series for the ORA-IP models is short and the positive correlations are only statistically significant at a few grid points in CGLORS and UR025.4, this behavior is sufficiently problematic to recommend that care should be taken when using these ORA-IP models to study the interannual variability in the Canadian Arctic.

In the CMIP5 models, significant winter snow depth trends are more strongly negative in the North than in the South (Figure 14). This is in disagreement with point observations presented in the previous sections that showed no significant trends snow depth trends at Alert but negative and significant trends at Cambridge Bay. Although only based on limited point *in situ* observations, this suggests that over the last decades changes in winter precipitation at Alert must have compensated the increased melting driven by increasing temperatures, a compensation that is clearly not captured in CMIP5 models..

5. Conclusions

Over the 50+ year in situ observational record, statistically significant negative trends in maximum (end-of-winter) ice thickness are present at Cambridge Bay, Eureka and Alert. Significant negative trends in the day of maximum ice thickness are also present at Resolute, Eureka and Alert. Together, these trends suggest thinning of landfast ice in the CAA, where little evidence was found in the shorter record analyzed in an earlier study (BC92). The inter-annual variability of air temperature is only weakly correlated to maximum ice thickness (i.e. maximum correlation is ~0.4). Snow thickness plays the dominant role in controlling maximum ice thickness variability given the high correlations at Resolute and Eureka and reasonably high correlations at Alert and Cambridge Bay.

Comparison of CMIP5, ORA-IP and PIOMAS simulations with observations indicate a reasonable representation of the landfast ice thickness monthly climatology within the CAA. This is particularly apparent when seasonal first-year ice dominates the icescape (i.e. Cambridge Bay). Despite improvements in spatial resolution, mixed ice types (i.e. seasonal and multi-year) present at the sub-grid cell resolution are likely problems for model estimates within the CAA. The overall thickness of ice within the CAA in the current generation of models is too high. As a result, trends are unrealistic and far exceed observations (by upwards of -50 cm decade^{-1}) in part because the initial ice thickness is too large. The problem is particularly acute in the ORA-IP models where large and unrealistic inter annual changes in thickness suggest that the models are not fully equilibrated.

While the impact of the snow cover on ice thickness is well known, the significant correlations at Resolute, Eureka and Alert suggest that the higher sensitivity to changes in snow depth could potentially mask the warming signal on both fast and offshore ice. Thus, even in this limited data set, we can see the dominant role played by snow depth in determining the

interannual variability of the maximum landfast ice thickness. This again highlights that the primary factor is the amount and timing of snow accumulation, not air temperature. However, it is worth noting that few of the current generation models show coherent relationships between ice thickness, snow depth and temperature over the longer term record.

Appendix

The Monte-Carlo simulation used to combine trends and Pearson correlations is applied at each grid point independently. Models that have a land mask at a grid point are discarded before starting the procedure.

A noise model is created to ensure that internal variability is comparable for models with different ensemble sizes, following Swart et al. [2014] and Laliberté et al. [2016]. To generate the noise model, we discard models that have fewer than two realizations. From the remaining models, we pick one and then one of its realizations. We then record to the noise model the difference of this realization's trend from the mean trend of the model's realizations, multiplied by $(n/(n-1))^{1/2}$, with n being the number of realizations, to account for the fact that some models have such a small number of realizations that it cannot completely account for the internal variability. We repeat this procedure 1000 times and compute the variance σn of the noise model.

We then pick a model from which we select 1000 realizations, allowing repetitions. For each one of these realizations, we select a random value from its trend t-distribution. If the inter-realization trend variance σ_m is smaller than the variance of the noise model σ_n, we then draw a random value from the noise model, multiply it by $(1-\sigma_m/\sigma_n)^{1/2}$ and add it to the random value from the trend t-distribution.

We repeat this procedure with the remaining models. We then average the 1000 values across models, creating a distribution for the multi-model mean trend with 1000 values. The mean of this distribution gives our multi-model mean and its two-sided p-value is given by twice its survival function or cumulative distribution function at 0, whichever is smallest.

The Pearson correlations are analyzed in the same way except that a Fisher transform (obtained by the hyperbolic arctangent of the correlation) is applied first and random values are drawn from a normal distribution (instead of the t-distribution) with variance 1/(T-3), with T the number of years used for the correlation. The multi-model mean Pearson correlation is then given by the inverse Fisher transform (obtained by the hyperbolic tangent of the mean) of the distribution mean.

Authors Contributions

S.E.L.H, F.L and R.K designed the study, performed the analysis and wrote the manuscript with input from C.D. and J.K.

Acknowledgements

The authors with to thank all the individuals responsible for collecting landfast ice and snow thickness measurements in the Canadian Arctic over the past 50+ years.

References

Alt, B., K. Wilson, and T. Carrieres (2006), A case study of old ice import and export through Peary and Sverdrup channels in the Canadian Arctic Archipelago: 1998-2004, *Ann. Glaciol*., 44, 329–338, doi:10.3189/172756406781811321.

M.A. Balmaseda , F. Hernandez , A. Storto , M.D. Palmer , O. Alves , L. Shi , G.C. Smith , T. Toyoda , M. Valdivieso , B. Barnier , D. Behringer , T. Boyer , Y-S. Chang , G.A. Chepurin , N.

Ferry , G. Forget , Y. Fujii , S. Good , S. Guinehut , K. Haines , Y. Ishikawa , S. Keeley , A. Köhl , T. Lee , M.J. Martin , S. Masina , S. Masuda , B. Meyssignac , K. Mogensen , L. Parent , K.A. Peterson , Y.M. Tang , Y. Yin , G. Vernieres , X. Wang , J. Waters , R. Wedd , O. Wang , Y. Xue , M. Chevallier , J-F. Lemieux , F. Dupont , T. Kuragano , M. Kamachi , T. Awaji , A. Caltabiano , K. Wilmer-Becker , F. Gaillard, The Ocean Reanalyses Intercomparison Project (ORA-IP), *Journal of Operational Oceanography*, Vol. 8, Iss. sup1, 2015, DOI:10.1080/1755876X.2015.1022329

Brown, R., and P. Cote (1992), Interannual variability of landfast ice thickness in the Canadian high arctic, 1950–89. *Arctic*, 45, 273–284.

Bromwich, D. H., A. B. Wilson, L. Bai, G. W. K. Moore, and P. Bauer, 2015: A comparison of the regional Arctic System Reanalysis and the global ERA-Interim Reanalysis for the Arctic. *Q. J. R. Meteorol. Soc*., doi: 10.1002/qj.2527

Dee DP, co-authors (2011), The ERA-Interim reanalysis: configuration and performance of the data assimilation system. *Q J R Meteorol Soc*. 137: 553–597, doi:10.1002/qj.828.

Dumas, J. A., G. M. Flato, and R. D. Brown (2006), Future projections of landfast ice thickness and duration in the Canadian Arctic. *J. Climate*, 19, 5175–5189.

Druckenmiller, M. L., H. Eicken, M. A. Johnson, D. J. Pringle, and C. C. Williams (2009), Toward an integrated coastal sea-ice observatory: System components and a case study at Barrow, Alaska. *Cold Reg.Sci.Tech*., 56, 61-72.

Flato, G. M., and R. D. Brown (1996),Variability and climate sensitivity of landfast Arctic sea ice. *J. Geophys. Res*., 101 (C10), 25 767–25 777.

Forget, G., Campin, J.-M., Heimbach, P., Hill, C. N., Ponte, R. M., and Wunsch, C. (2015), ECCO version 4: an integrated framework for non-linear inverse modeling and global ocean state estimation, *Geosci. Model Dev*., 8, 3071-3104, doi:10.5194/gmd-8-3071-2015/

Gerland, S., A. H. H. Renner, F. Godtliebsen, D. Divine, and T. B. Loyning (2008), Decrease of sea ice thickness at Hopen, Barents Sea, during 1966-2007. *Geophys. Res. Lett*., 35, L06501.

Gough, W., A.S. Gagnon an H.P Lau (2004), Interannual variability of Hudson Bay Ice Thickness, *Polar Geography*, 28(3), 222-238.

Haines K, M. Valdivieso, H. Zuo, and V.N. Stepanov (2012), Transports and budgets in a 1/4 ° global ocean reanalysis 1989–2010. *Ocean Sci.* 8(3): 333–344, doi:10.5194/os-8-333-2012.002/qj.2063.

Haas, C., and S. E. L. Howell (2015), Ice thickness in the Northwest Passage, *Geophys. Res. Lett.*, 42, doi:10.1002/2015GL065704

Howell, S. E. L., C. R. Duguay, and T. Markus (2009), Sea ice conditions and melt season duration variability within the Canadian Arctic Archipelago: 1979–2008, Geophys. Res. Lett., 36, L10502, doi:10.1029/2009GL037681.

Howell, S. E. L., T. Wohlleben, M. Dabboor, C. Derksen, A. Komarov, and L. Pizzolato (2013), Recent changes in the exchange of sea ice between the Arctic Ocean and the Canadian Arctic Archipelago, *J. Geophys. Res. Oceans*, 118, 3595–3607, doi:10.1002/jgrc.20265.

Jeffers, S., T. Agnew, B. Alt, R. De Abreu, and S. McCourt (2001), Investigating the anomalous sea ice conditions in the Canadian High Arctic (Queen Elizabeth Islands) during the summer of 1998, *Ann. Glaciol*., 33, 507– 612.

Jeffries, M. O. and J. Richter-Menge, Eds. (2015), The Arctic [in State of the Climate in 2014], *Bull. Amer. Meteor. Soc*., 96, ES1–ES32.
doi: http://dx.doi.org/10.1175/2015BAMSStateoftheClimate.1

Jones, P.D., T.M.L. Wigley, C.K. Folland and D.E. Parker (1987), Spatial patterns in recent worldwide temperature trends. *Climate Monitor*, 16(5): 175-185.

Jones, P.D., M. New, D.E. Parker, S. Martin, and I.G. Rigor (1999), Surface air temperature and its changes over the past 150 years, *Rev. Geophys*, 37(2),173–200.

Kwok, R., and D. A. Rothrock (2009), Decline in Arctic sea ice thickness from submarine and ICESat records: 1958 – 2008, *Geophys. Res. Lett*., 36, L15501, doi:10.1029/2009GL039035.

Laliberté, F., S. E. L. Howell, and P. J. Kushner (2016), Regional variability of a projected sea ice-free Arctic during the summer months, *Geophys. Res. Lett*., 43, 256–263, doi:10.1002/2015GL066855.

Laxon S. W., K. A. Giles, A. L. Ridout, D. J. Wingham, R. Willatt, R. Cullen, R. Kwok, A. Schweiger, J. Zhang, C. Haas, S. Hendricks, R. Krishfield, N. Kurtz, S. Farrell and M. Davidson (2013), CryoSat-2 estimates of Arctic sea ice thickness and volume, *Geophys. Res. Lett*., 40, 732–737, doi:10.1002/grl.50193.

Masina, S. et al. (2015), An ensemble of eddy-permitting global ocean reanalyses from the MyOcean project. *Clim. Dynam*. 1–29, doi:10.1007/s00382-015-2728-5

Mahoney, A., H. Eicken, and L. Shapiro (2007), How fast is landfast sea ice? A study of the attachment and detachment of nearshore ice at Barrow, Alaska. *Cold Reg.Sci.Tech*., 47, 233-255.

Mahoney, A. R., H. Eicken, A. G. Gaylord, and R. Gens (2014), Landfast sea ice extent in the Chukchi and Beaufort seas: The annual cycle and decadal variability, Cold Reg. Sci. Technol. , 103, 41–56, doi:10.1016/j.coldregions.2014.03.003.

Melling, H. (2002), Sea ice of the northern Canadian Arctic Archipelago, *J. Geophys. Res*., 107(C11), 3181, doi:10.1029/2001JC001102.

Melling, H., C. Haas, and E. Brossier (2015), Invisible polynyas: Modulation of fast ice thickness by ocean heat flux on the Canadian polar shelf, *J. Geophys. Res. Oceans*, 120, 777–795, doi:10.1002/2014JC010404.

Ólason, E. Ö. (2012), Dynamical modeling of Kara Sea land-fast ice, PhD thesis, Univ. of Hamburg, Hamburg, Germany.

Polyakov, I. V., et al. (2010), Arctic Ocean Warming Contributes to Reduced Polar Ice Cap. *Journal of Physical Oceanography*, 40, 2743-2756

Schweiger, A., R. Lindsay, J. Zhang, M. Steele, H. Stern, and R. Kwok (2011), Uncertainty in modeled Arctic sea ice volume, *J. Geophys. Res*., 116, C00D06, doi:10.1029/2011JC007084.

Serson, H.V. (1972), Investigations of a plug of multiyear old sea icein the mouth of Nansen Sound. Ottawa, Ont., Department of National Defence, Canada. Defence Research Establishment Ottawa. (DREO Tech. Note 72-6.)

Serson, H.V. (1974), Sverdrup Channel. Ottawa, Ont., Department of National Defence, Canada. Defence Research Establishment Ottawa. (DREO Tech. Note 74-10.)

Sou, T., and G. Flato (2009), Sea ice in the Canadian Arctic Archipelago: Modeling the past (1950-2004) and the future (2041-60), J. Clim., 22, 2181–2198, doi:10.1175/2008JCLI2335.1

Stroeve, J. C., M. C. Serreze, M. M. Holland, J. E. Kay, J. Malanik, and A. P. Barrett (2011), The Arctic's rapidly shrinking sea ice cover: A research synthesis, *Clim. Change*, 110(3-4), 1005–1027.

Storto A, S. Dobricic S, S. Masina and D. Di Pietro (2011), Assimilating along-track altimetric observations through local hydrostatic adjustments in a global ocean reanalysis system. *Mon Wea Rev*. 139: 738–754.

Stroeve, J. C., M. C. Serreze, M. M. Holland, J. E. Kay, J. Maslanik, and A. P. Barrett (2012), The Arctic's rapidly shrinking sea ice cover: A research synthesis, *Clim. Change*, 110(3–4), 1005–1027

Swart, N. C., J. C. Fyfe, E. Hawkins, J. E. Kay, and A. Jahn (2015), Influence of internal variability on Arctic sea-ice trends, *Nat. Clim. Change*, 5, 86–89, doi:10.1038/nclimate2483.

Taylor, K. E., R. J. Stouffer, and G. A. Meehl (2012), An overview of CMIP5 and the experiment design, *Bull. Am. Meteorol. Soc*., 93, 485–498, doi:10.1175/BAMS-D-11-00094.1.

Tivy, A., S. E. L. Howell, B. Alt, S. McCourt, R. Chagnon, G. Crocker, T. Carrieres, and J. J. Yackel (2011), Trends and variability in summer sea ice cover in the Canadian Arctic based on the Canadian Ice Service Digital Archive, 1960–2008 and 1968–2008, *J. Geophys. Res*., 116, C03007, doi:10.1029/2009JC005855.

Vincent, L., X. Wang, E. Milewska, Hui Wan, F. Yang, and V. Swail (2012), A second generation of homogenized Canadian monthly surface air temperature for climate trend analysis. *Journal of Geophysical Research*, D18110, doi:10.1029/2012JD017859

Warren, S. G., I. G. Rigor, N. Untersteiner, V. F. Radionov, N. N. Bryazgin, Y. I. Aleksandrov, and R. Colony (1999), Snow depth on Arctic sea ice, *J. Clim*., 12, 1814– 1829.

Wilks, D. S. (2006). On "field significance" and the false discovery rate. *J. Appl. Meteor. Climatol*., 45, 1181–1189. doi: http://dx.doi.org/10.1175/JAM2404.1

Woo, M-K., and R. Heron (1989), Freeze-up and break-up of ice cover on small arctic lakes. In: Mackay, W.C., ed. Northern lakes and rivers. Edmonton: Boreal Institute for Northern Studies, 56-62.

Woo, M-K., R. Heron, P. Marsh, and P. Steer, (1983), Comparison of weather station snowfall with winter snow accumulation in High Arctic basins, *Atmos.-Ocean*, 21(3):312-325.

World Meteorological Organization, (1970), WMO sea-ice nomenclature. Terminology, codes and illustrated glossary. WMO/OMM.BMO No. 259, 145 pp, Geneva Secretariat of the World Meteorological Organization

Yu, Y, H. Stern, C. Fowler, F. Fetterer, and J. Maslanik (2014), Interannual Variability of Arctic Landfast Ice between 1976 and 2007. *J. Climate*, **27**, 227–243. doi: http://dx.doi.org/10.1175/JCLI-D-13-00178.1

Zhang, J.L. and D.A. Rothrock, (2003), Modeling global sea ice with a thickness and enthalpy distribution model in generalized curvilinear coordinates, *Mon. Weather Rev*., 131, 845-861.

Zuo, H., M.A. Balmaseda, and K. Mogensen (2015), The new eddy-permitting ORAP5 ocean reanalysis: description, evaluation and uncertainties in climate signals. *Clim. Dynam*. 1–21. doi:10.1007/s00382-015-2675-1.

Table 1. CMIP5 models used in this study, the number of realizations with ice data and the number of realizations with sea ice transport data

	w/ ice		w/ ice
bcc-csm1-1	1	MIROC-ESM-CHEM	1
bcc-csm1-1-m	1	MIROC5	3
BNU-ESM	1	HadGEM2-CC	1
CanESM2	5	HadGEM2-ES	4
CMCC-CESM	1	MPI-ESM-LR	3
CMCC-CM	1	MPI-ESM-MR	1
CMCC-CMS	1	MRI-CGCM3	1
CNRM-CM5	5	CCSM4	6
ACCESS1.0	1	NorESM1-M	1
ACCESS1.3	1	NorESM1-ME	1
CSIRO-Mk3.6.0	10	GFDL-CM3	1
FIO-ESM	1	GFDL-ESM2G	1
EC-EARTH	6	GFDL-ESM2M	1
inmcm4	1	CESM1(BGC)	1
FGOALS-g2	1	CESM1(CAM5)	3
MIROC-ESM	1	CESM1(WACCM)	3

Table 2. Summary of ORA-IP models characteristics

Model Name	CGLORS	ECCO-v4	GLORYS2V3	ORAP5.0	UR025.4	PIOMAS
Institute	CMCC	JPL-NASA-MIT-AER	Mercator Océan	ECMWF	University of Reading	APL/PSC
Resolution	ORCA0.25°	~40km in the Arctic	ORCA0.25°	ORCA0.25°	ORCA0.25°	~22km in the Arctic
Ocean Model	NEMO 3.2.1	MITgcm	NEMO 3.1	NEMO3.4	NEMO 3.2	POP
Sea ice Model	LIM2	MITgcm	LIM2 (with EVP rheology)	LIM2	LIM2	TED
Time period considered	1982-2012	1991-2011	1993-2013	1985-2013	1993-2010	1958-2015
Atmospheric forcing	ERA-Interim	ERA-Interim	ERA-Interim	ERA-Interim	ERA-Interim	NCEP/NCAR
Sea ice product assimilated	NSIDC NASA-Team Daily	NSIDC Bootstrap Monthly	IFREMER/CERSAT	NOAA / OSTIA combination	EUMETSAT OSI-SAF	NSIDC near-real time Daily

Table 3. Observed maximum ice thickness, snow depth, and surface air temperature at four landfast ice sites in the Canadian Arctic Archipelago. The bold text indicates statistical significance of the linear trend at 95% or greater.

	Cambridge Bay	Resolute	Eureka	Alert
Period	1960-2014	1957-2014	1957-2014	1957-2014
Ice Thickness, h_{ice}				
Mean of *max* h_{ice} (m)	2.11±0.19	2.02±0.19	2.27±0.23	1.98±0.22
Trend of *max* h_{ice} (cm decade^{-1})	**-4.31±1.4**	-0.5±1.6	**-4.65±1.7**	**-4.44±1.6**
Day of *max* h_{ice}	24 May±17	25 May±21	26 May±12	27 May±16
Trend of day of *max* h_{ice} (days decade^{-1})	-0.87±1.5	**-6.2±1.5**	**-2.0±0.1**	**-3.0±1.2**
Snow depth (h_{snow})				
Mean Oct-May h_{snow} (cm)	8.4±4.2	22.6±10	17.6±5.8	18.4±6.2
Trend of Oct-May h_{snow} (cm decade^{-1})	**-0.8±0.4**	-0.75±0.8	0.54±0.5	0.26±0.5
Temperature				
Winter (Dec-Feb) Mean (^{o}C)	-31.3±2.0	-30.8±1.9	-36.0±2.0	-31.2±1.6
Winter (Dec-Feb) (^{o}C/decade)	**0.59±0.2**	**0.35±0.1**	0.23±0.2	**0.38±0.1**
Spring (Mar-May) Mean (^{o}C)	-20.0±1.8	-21.1±1.8	-24.9±2.0	-22.8±1.8
Spring (Mar-May) (^{o}C/decade)	**0.47±0.1**	**0.57±0.1**	**0.44±0.1**	**0.32±0.1**
Summer (Jun-Aug) Mean (^{o}C)	5.9±1.4	2.3±1.3	3.9±1.2	1.3±0.8
Summer (Jun-Aug) (^{o}C/decade)	**0.30±0.1**	0.17±0.2	**0.21±0.1**	**0.1±0.1**
Fall (Sep-Nov) Mean (^{o}C)	-11.1±2.0	-13.8±2.0	-19.6±2.2	-18.0±1.7
Fall (Sep-Nov) (^{o}C/decade)	**0.60±0.2**	**0.67±0.1**	**0.68±0.2**	**0.56±0.1**

List of Figures

Figure 13. **a-e:** Pearson correlation of detrended maximum sea ice thickness in ORA-IP with detrended ONDJFMAM ERA-INTERIM 2m temperature. **f:** Same but for CMIP5 MODEL-MEAN. The stippling indicates p-values less than 0.05, corrected using the False Discovery Rate (FDR) method with a global pFDR-values less than 0.10 [*Wilks*, 2006].

Figure 14. Same as Figure 12f but for snow depth trends (ONDFJMAM).

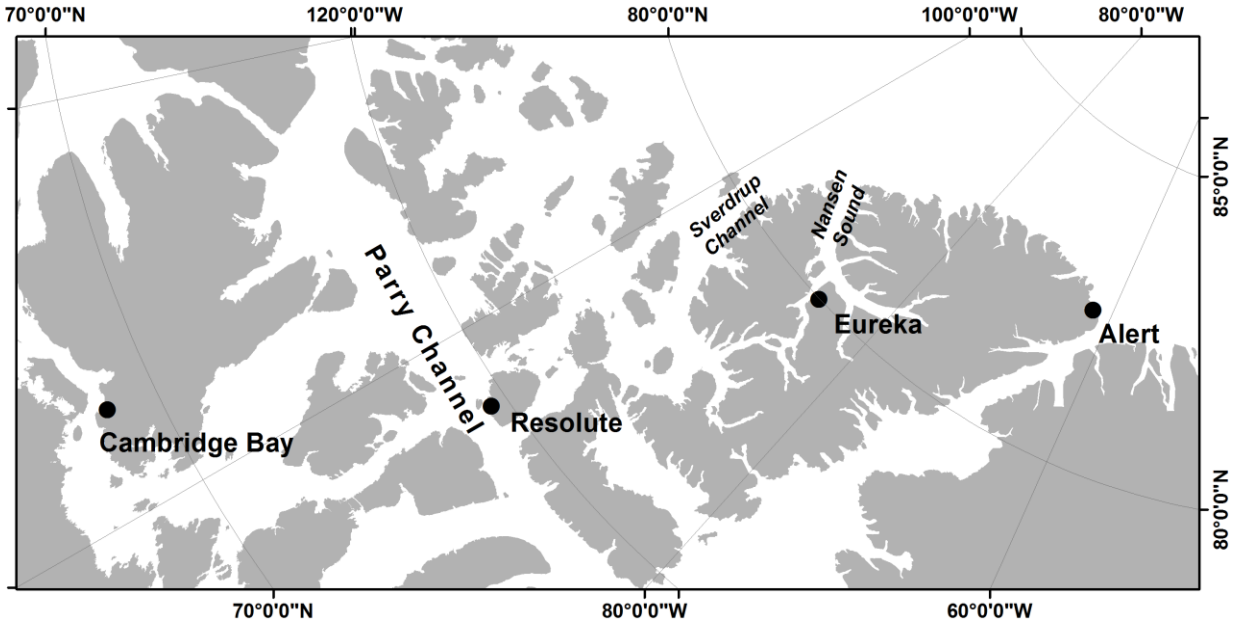

Figure 1. Map of the central Canadian Arctic Archipelago showing the location of the landfast snow and thickness observations.

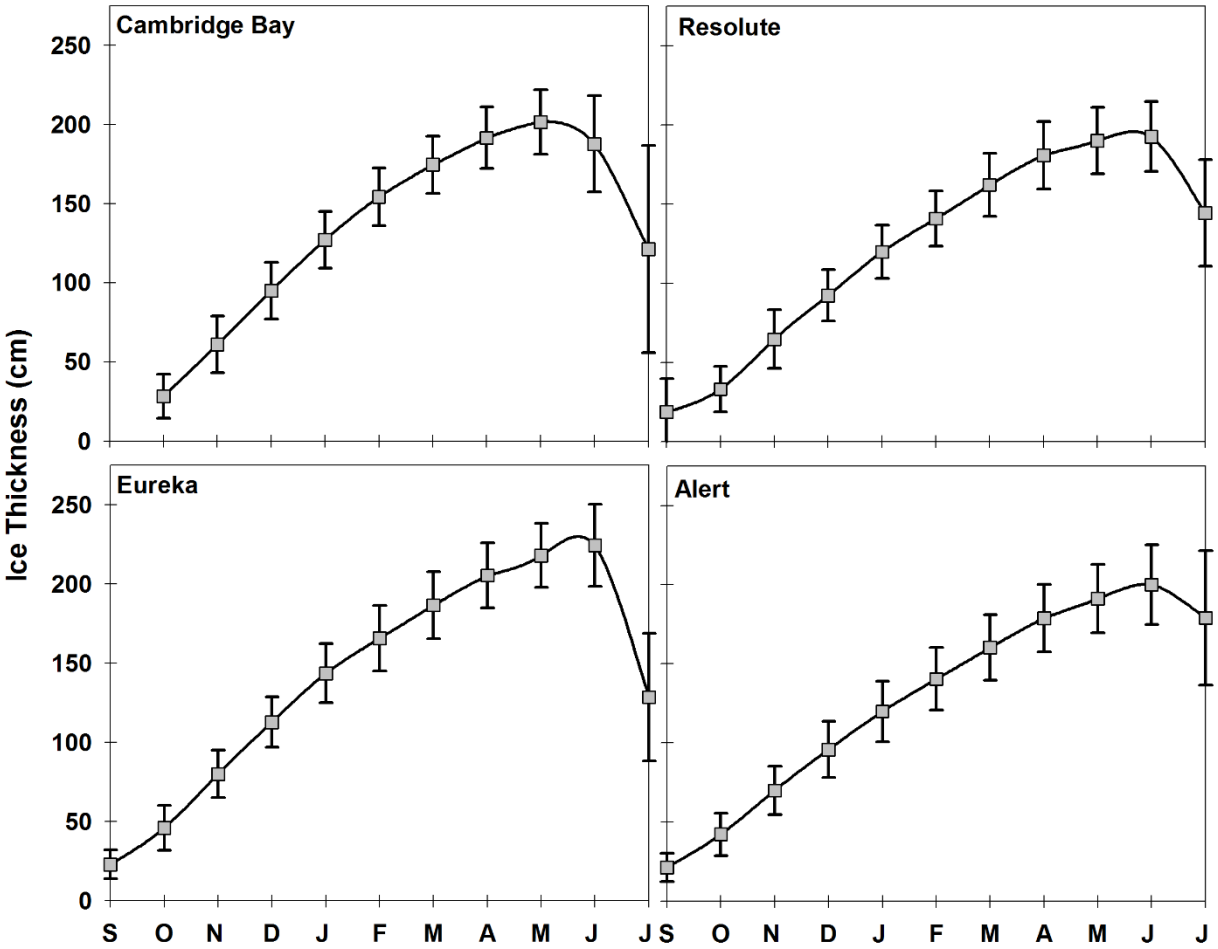

Figure 2. Seasonal cycle of observed mean ice thickness at the four sites (1960-2014).

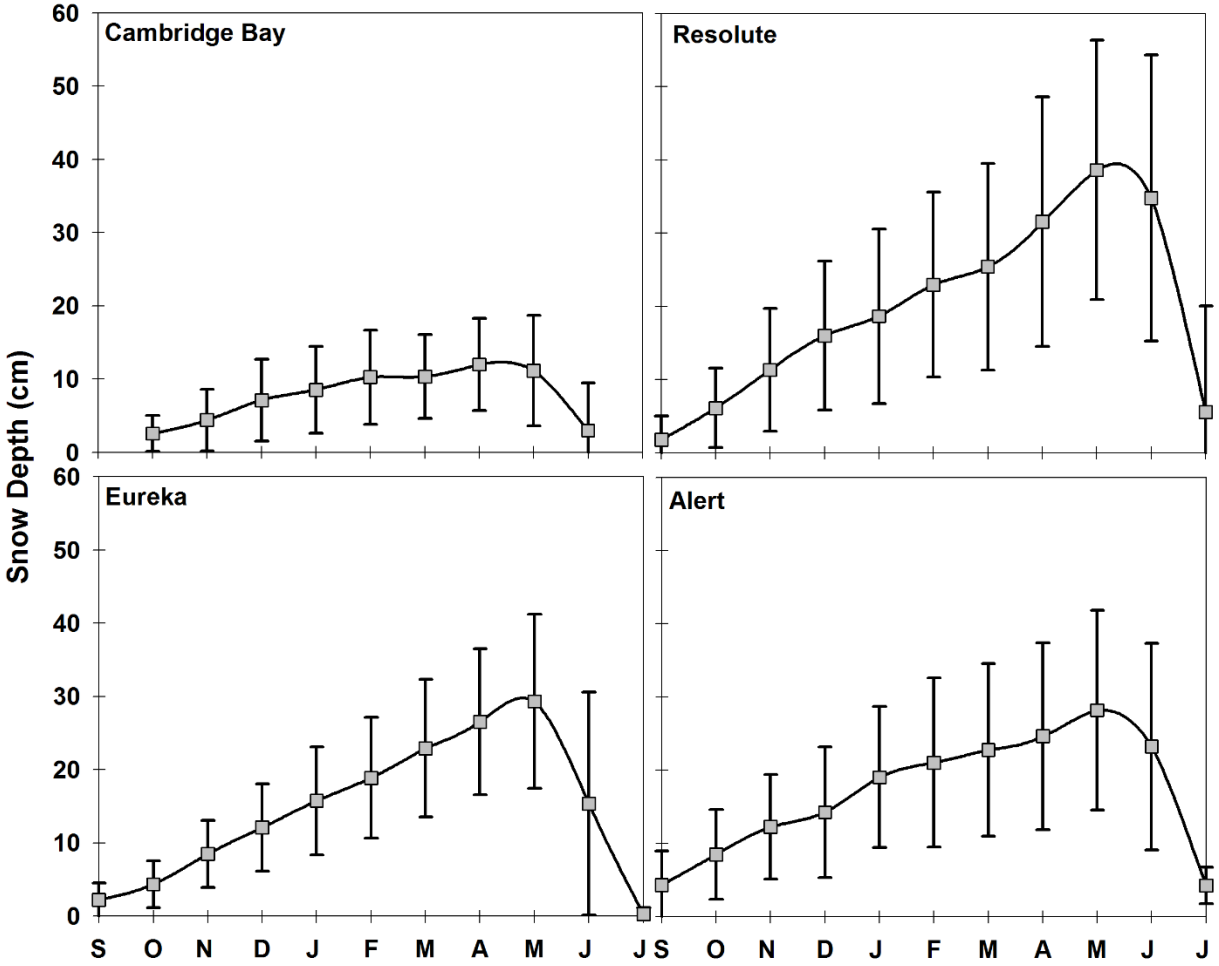

Figure 3. Seasonal cycle of observed mean snow depth at the four sites (1960-2014).

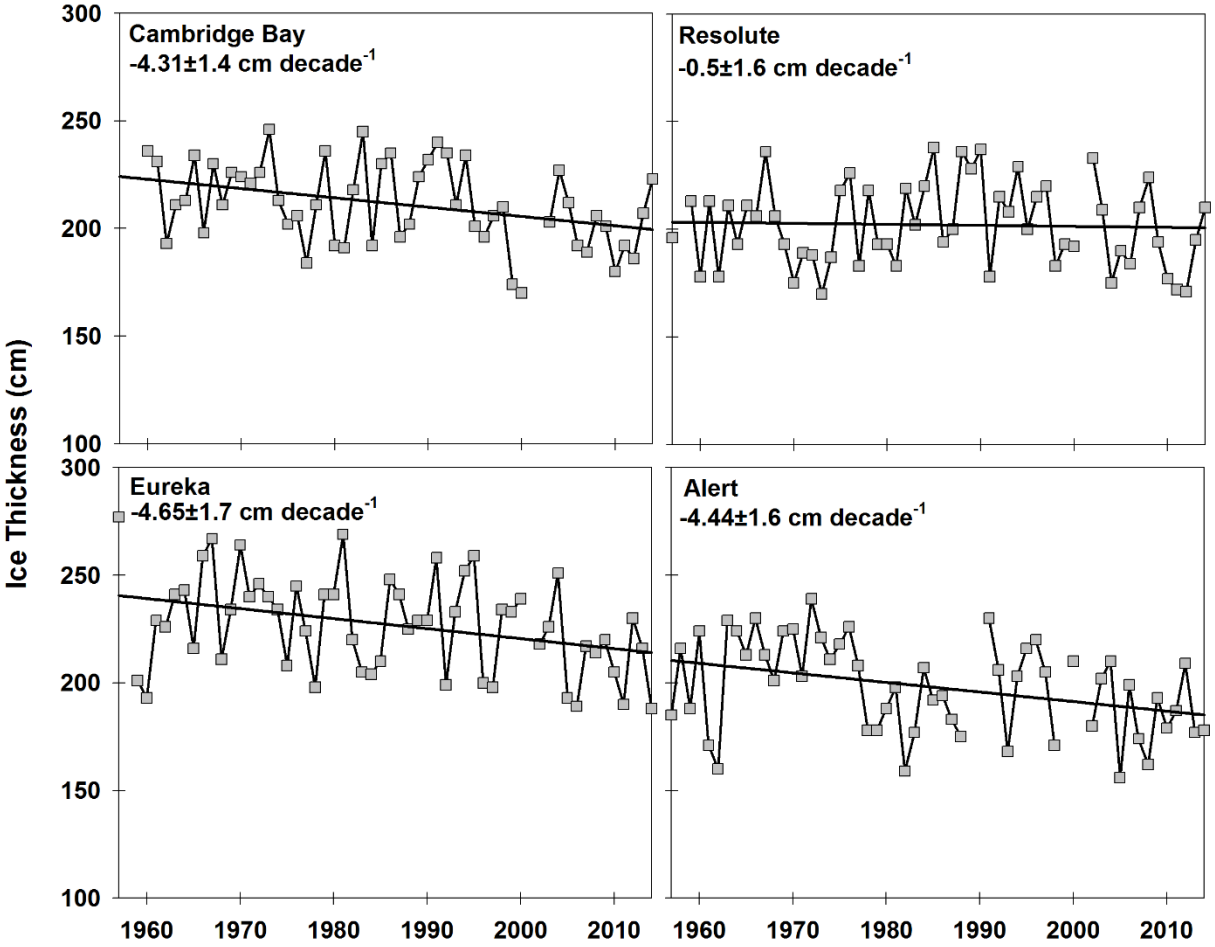

Figure 4. Time series and trend of observed maximum ice thickness at the four sites.

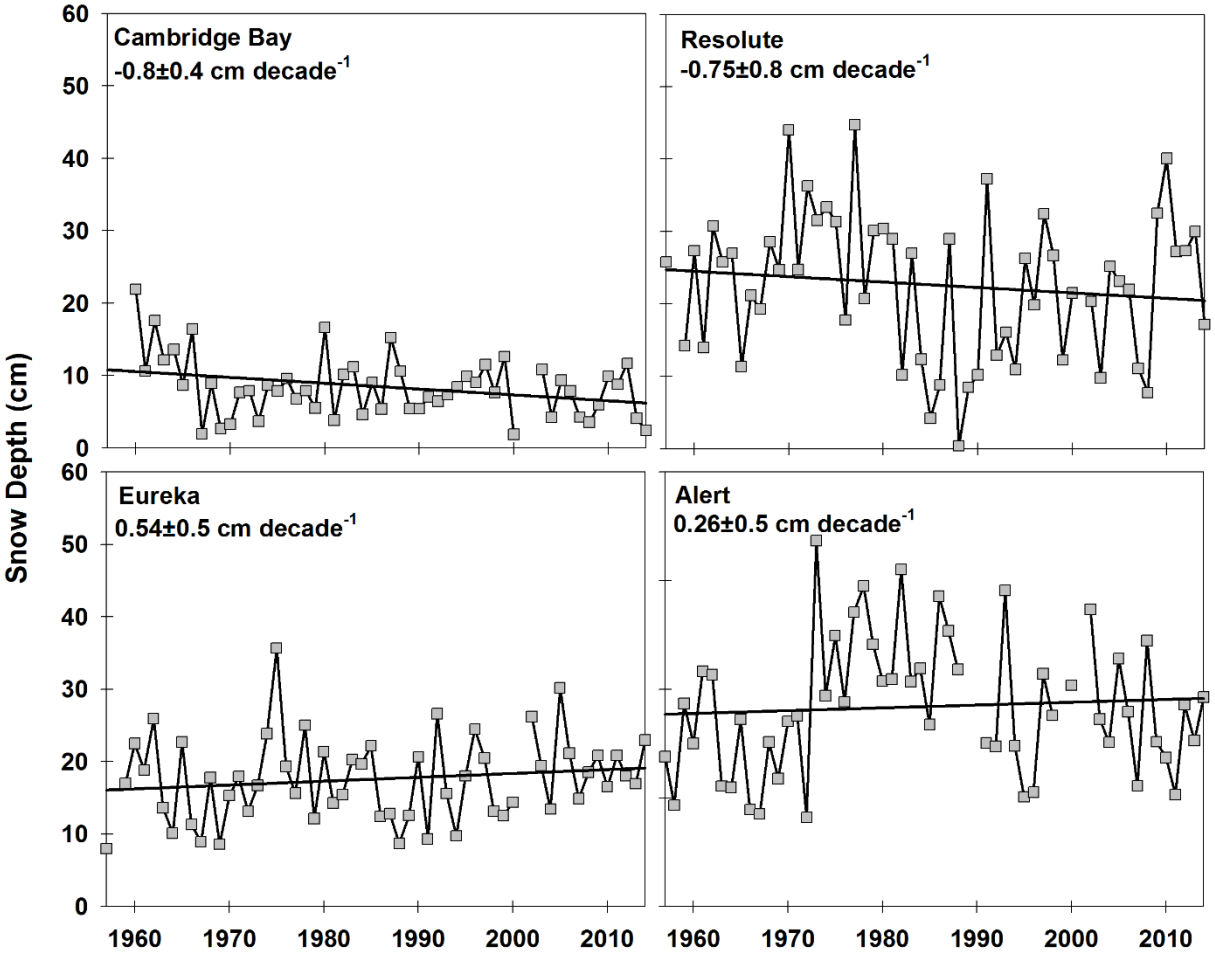

Figure 5. Time series and trend of observed mean October through May snow depth at the four sites.

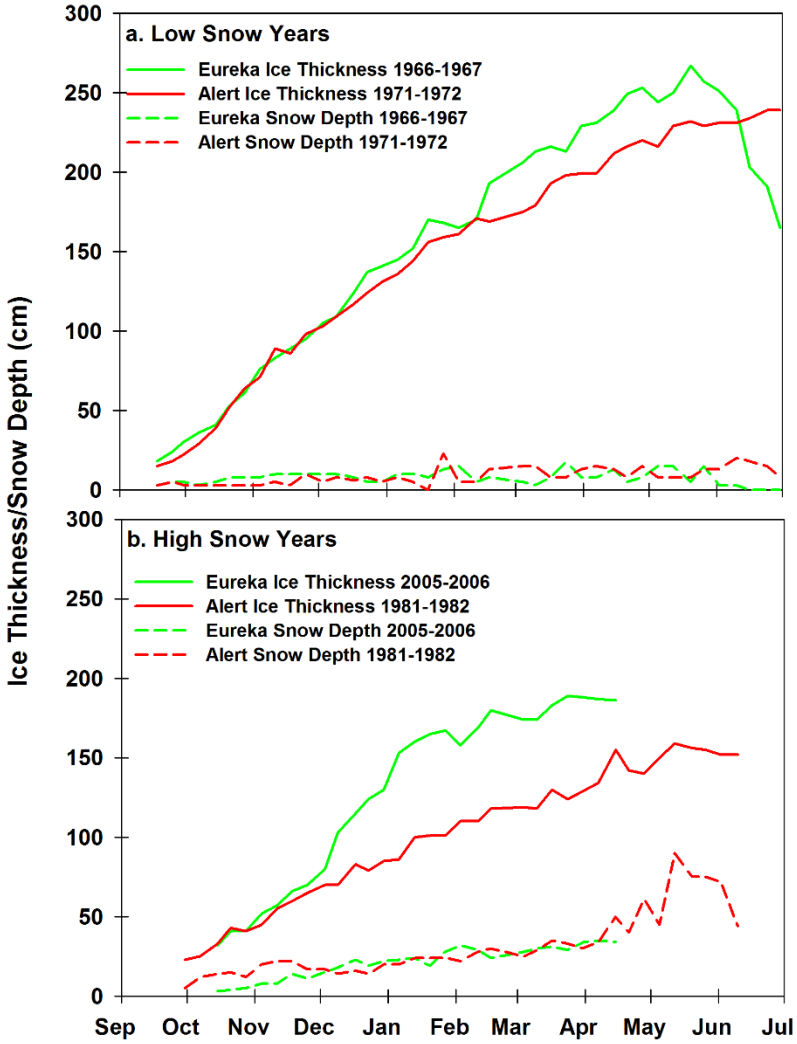

Figure 6. Weekly time series of ice thickness and snow depth at Eureka and Alert for (a) low snow years and (b) high snow years.

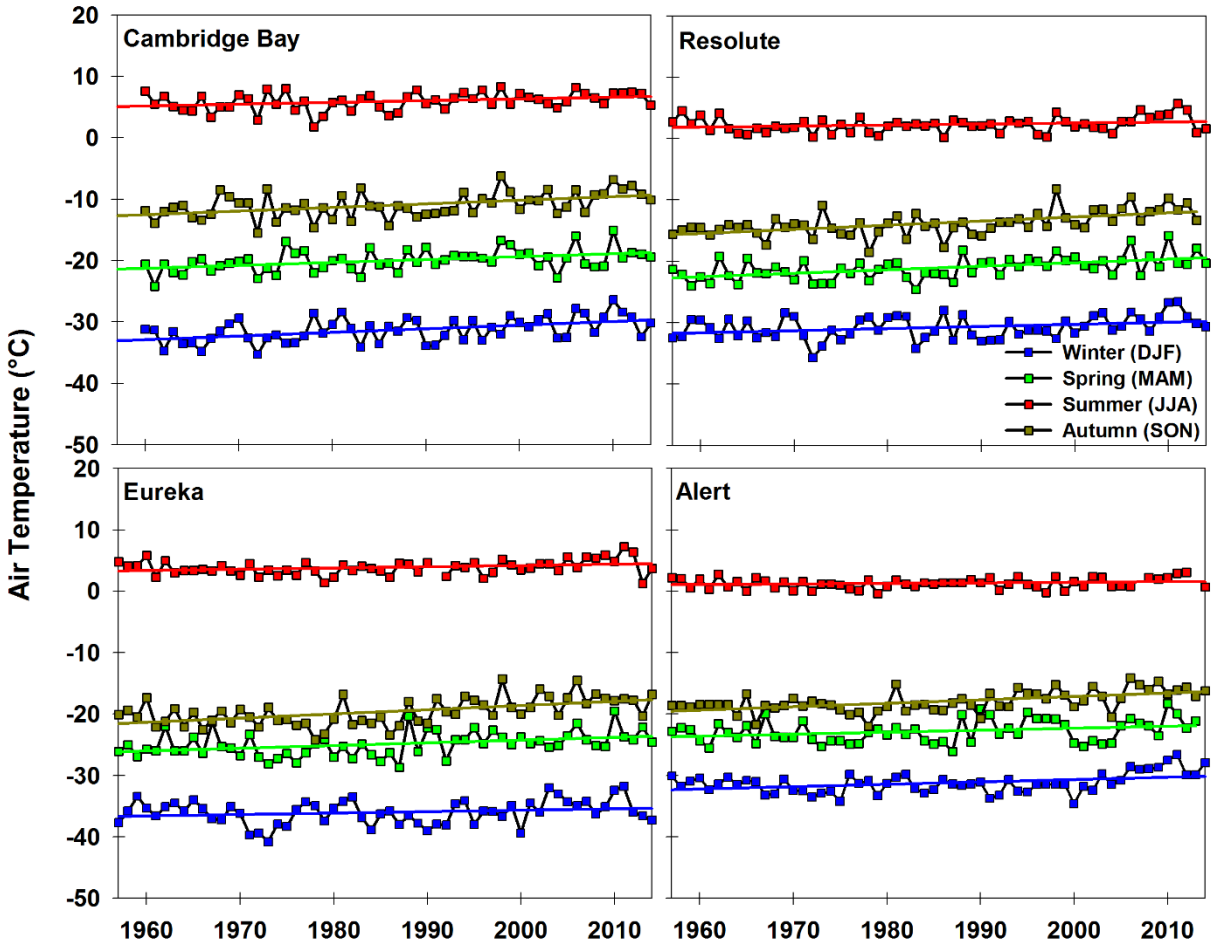

Figure 7. Time series observed mean air temperature by Environment Canada during winter (DFJ), spring, (MAM), summer (JJA) and autumn (SON) at the Cambridge Bay, Resolute, Eureka and Alert.

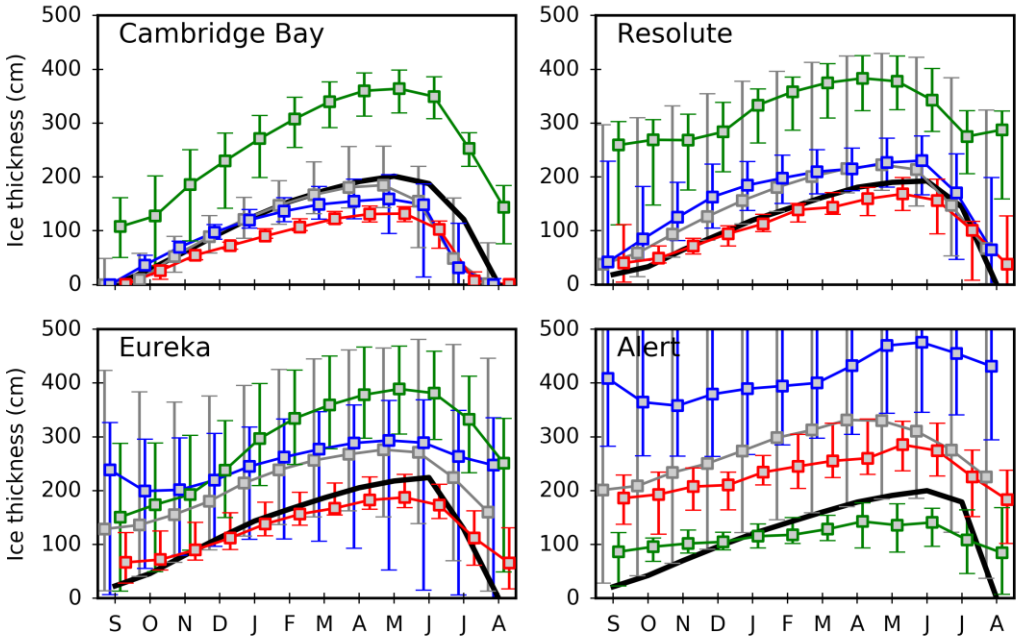

Figure 8. CMIP5 median sea ice thickness seasonal cycle (1955-2014) at stations (grey). Observations from 2 (black). Median of ORA-IP models CGLORS, ORAP5.0, GLORYS2V3 (blue), ECCO-v4 (green) and UR025.4 (red). Whiskers indicate the 5th and 95th percentiles.

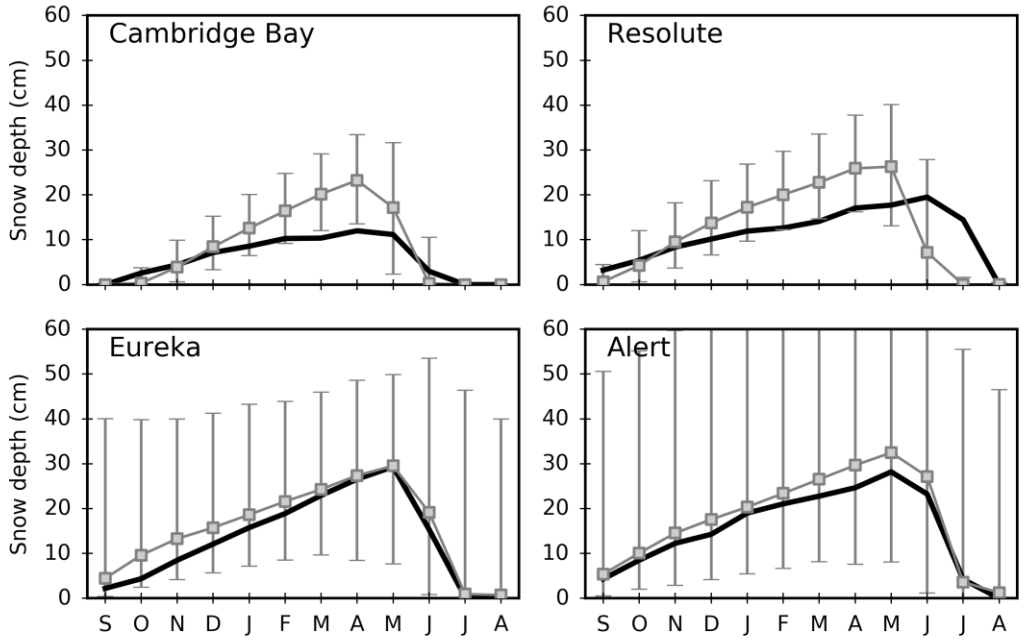

Figure 9. Same as Figure 8 for snow depth and only for CMIP5 models (grey) and observations (black).

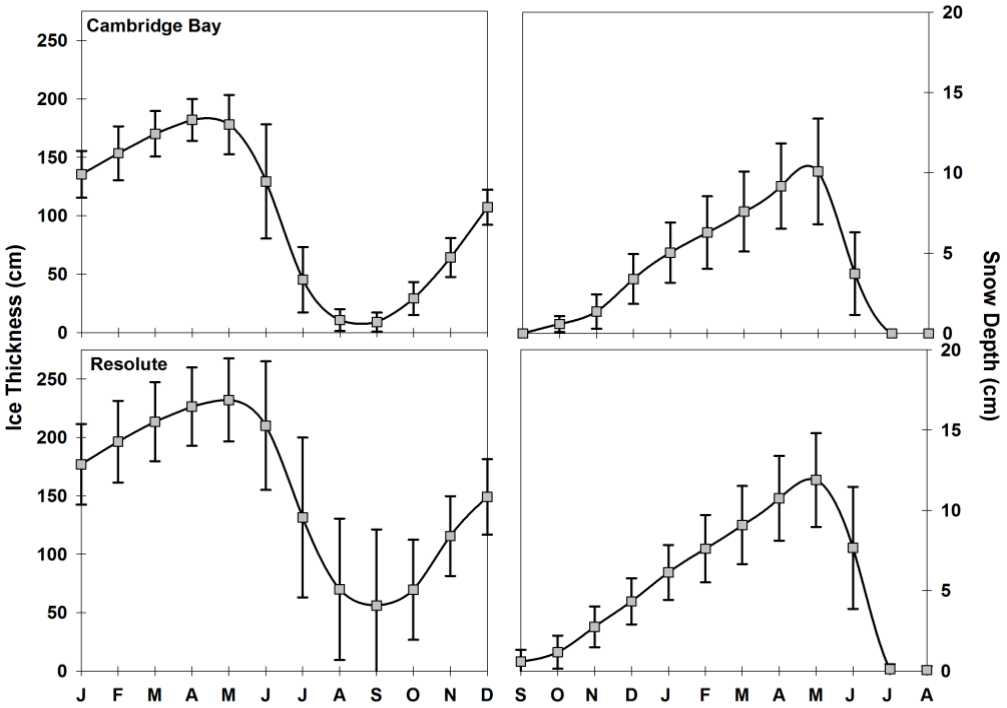

Figure 10. Seasonal cycle of observed mean ice thickness (left) and snow depth (right) from PIOMAS at Cambridge Bay and Resolute (1979-2014).

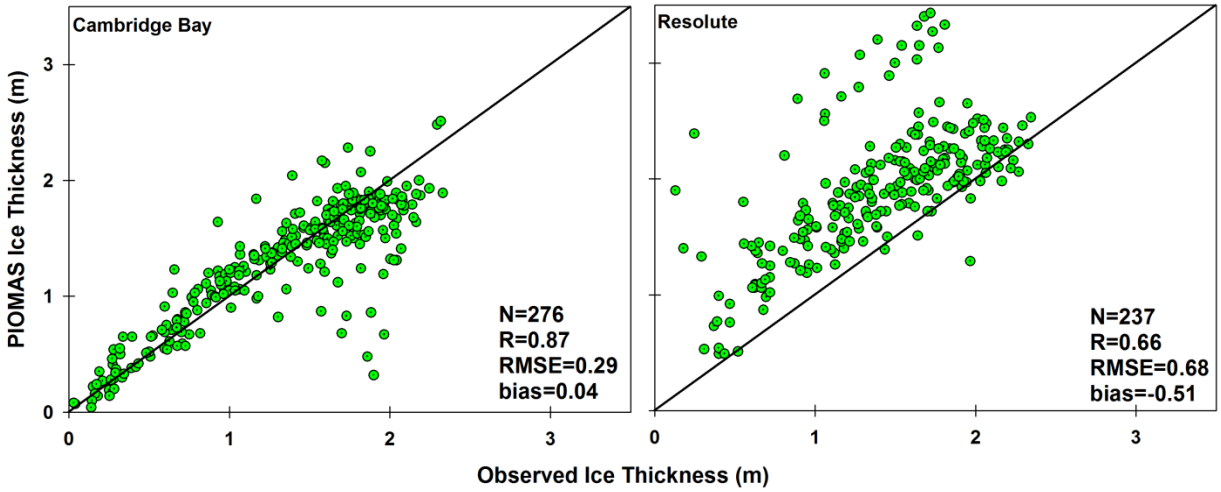

Figure 11. Comparison of PIOMAS ice thickness with ice thickness observations from Environment Canada's ice thickness monitoring sites at Cambridge Bay and Resolute. The data covers the period 1979-2014.

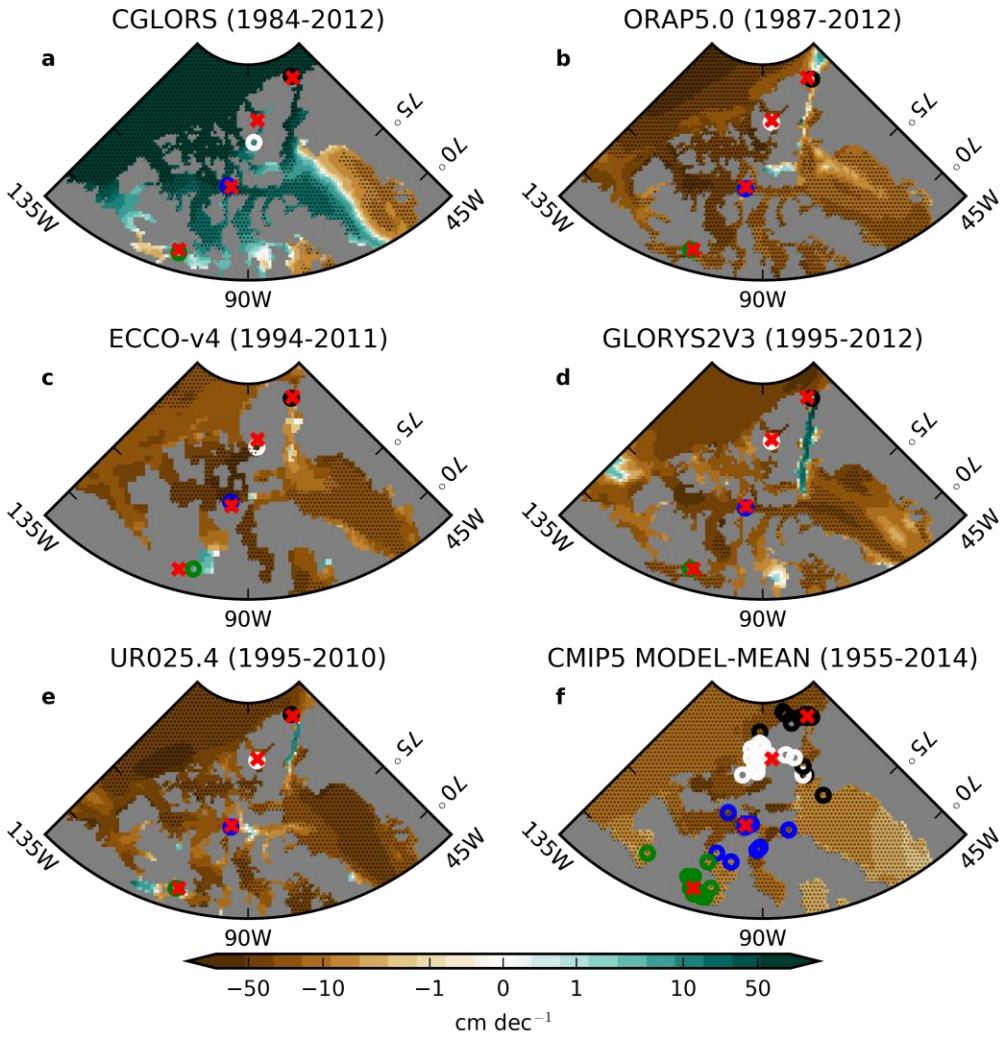

Figure 12. **a-e:** Maximum sea ice thickness trends in ORA-IP simulations. **f:** Same for CMIP5 MODEL-MEAN. From South to North, o's indicate Cambridge Bay (green), Resolute (blue), Eureka (white) and Alert (black) and x's indicate the corresponding measurement stations. In f, one o per model is shown." The stippling indicates p-values less than 0.05, corrected using the False Discovery Rate (FDR) method with a global pFDR-values less than 0.10 [*Wilks*, 2006]. The colorbar is linear from -10 cm dec^{-1} to 10 cm dec^{-1} and symmetric logarithmic beyond these values.

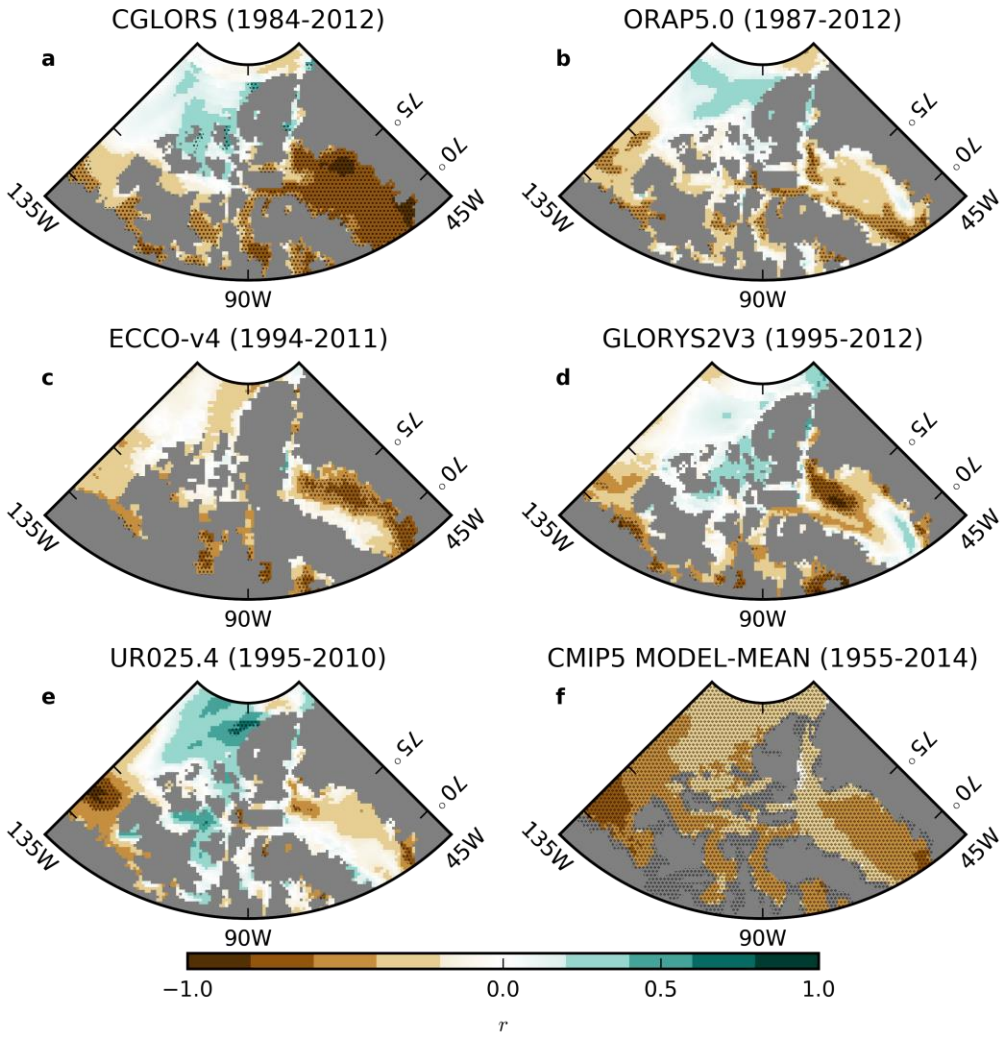

Figure 13. **a-e:** Pearson correlation of detrended maximum sea ice thickness in ORA-IP with detrended ONDJFMAM ERA-INTERIM 2m temperature. **f:** Same but for CMIP5 MODEL-MEAN. The stippling indicates p-values less than 0.05, corrected using the False Discovery Rate (FDR) method with a global pFDR-values less than 0.10 [*Wilks*, 2006].

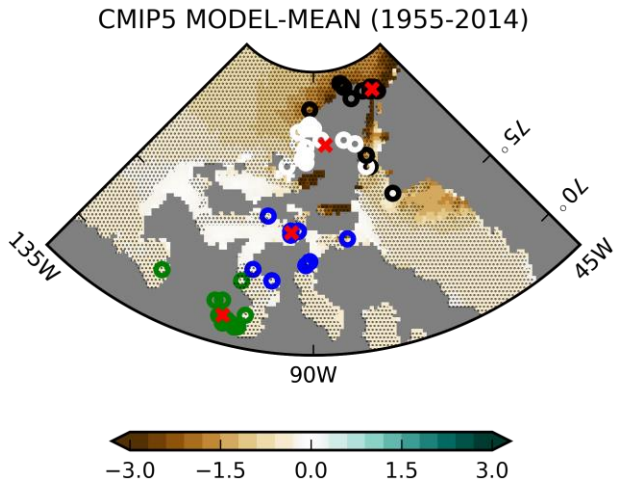

Figure 14. Same as Figure 12**f** but for snow depth trends (ONDFJMAM).